Journal of Applied Fluid Mechanics, Vol. 9, Special Issue 2, pp. 197-205, 2016.
Selected papers from *the XIIth Franco - Quebec Inter-University Symposiumon Thermal Systems -2015*
Available online at www.jafmonline.net, ISSN 1735-3572, EISSN 1735-3645.
DOI: 10.36884/jafm.9.SI2.25789

1D Steady-State Numerical Results for Critical Two-Phase Flow – Critical Location and Pressure Profiles

S. Martel[1†], M. Dostie[1] and Y. Mercadier[2]

[1] *Research Institut of Hydro-Quebec, Shawinigan, Quebec, G9N 7N5, Canada*
[2]*University of Sherbrooke, Sherbrooke, Quebec, J1K 2R1, Canada*

†*Corresponding Author Email: martel.sylvain@lte.ireq.ca*

(Received October 8, 2015; accepted December 10, 2015)

ABSTRACT

The use of two-phase ejectors to improve refrigeration systems encounters today a great interest. However, modeling of such devices with low void fraction at the entrance of the motive nozzle, presents significant challenges. The choking conditions and the discontinuities appearing in a two-phase flow in a nozzle are not well documented and some works are needed to better anticipated flow behavior under these conditions. This paper presents a steady state two-phase flow model including new choking criterions for one-dimensional conservative systems. The present model is a two-fluid, one pressure model with thermal equilibrium and mechanical disequilibrium. As a first step, this model is used to study the flow in the motive nozzle of an ejector.

Keywords: Two phase flow; Critical flow; Critical location; Nozzle flow.

NOMENCLATURE

A	nozzle section area
A_c	droplet section area
A_n	droplet surface
C_p	specific heat
e	internal energy
E	energy flux
F	external forces
f_{Ek}	enthalpy ratio in energy equation
f_{Ep}	pressure ratio in energy equation
f_{Eu}	velocity ratio in energy equation
f_{Jp}	pressure ratio
f_{Ju}	momentum ratio
f_M	mass flow rate ratio
g	gravitationnal force
h	enthalpy
h_c	heat transfer coefficient
h_y	enthalpy of vaporization
h_m	mass transfer coefficient
J	momentum flux
M	mass flux
n	normal vector
N	droplet flow
p	pressure
q	heat exchange
R	gas constant
s	slip ratio
t	time
T	temperature
u	velocity
V	volume
z_c	compressibility factor

Greek letters :

α	void fraction of phase
Γ	source term
ψ	a quantity of phase
φ	volumic term
ρ	density
ρ_s	saturation density
ρ_y	gas density
τ	train tensor

Subscripts / Superscripts :

c	boundary term
D	interfacial bourndary
E	energy term
Eu	kinetic transfer
Eq	convectiv transfer
Eh	enthalpy transfer
J	momentum term
k	phase
kf	boundary term
M	mass term
0	reference term, initial value
$1,2$	phase 1,2

1. INTRODUCTION

The steady state flow of compressible fluid through convergent-divergent nozzle covers various important flow phenomena like the occurrence of critical flow conditions, transition from subsonic to supersonic flow or the occurrence of flow discontinuities. For single-phase gas, relatively simple algebraic solutions exist as described in many gasdynamic textbooks. For two-phase flow conditions, iterative algebraic solutions can be derived only for simple one-dimensional case with homogeneous assumption and thermo-mechanical equilibrium between phases. For the more general case of nonhomogeneous and disequilibrium conditions, the numerical resolution present a major challenge.

In fact, several mathematical models have been published in the literature for two-phase flows but only a few have addressed the steady state behavior in a nozzle, especially with low void fraction, heat and mass transfer between phases, and phase interaction. In addition, two-phase critical flow has been the subject of many analytical and experimental investigations, mainly because of its importance in the safety analyses of pressurized water in nuclear reactors and converging-diverging nozzles.

One phenomena still of interest is the choking condition in a critical flow such as in supersonic ejectors. Supersonic ejectors are widely used in a range of applications such as aerospace, propulsion, refrigeration and many thermal systems. In refrigeration applications, ejectors could be used as thermo compressor or to recover part of the work that would be lost in the expansion valve. The flow at the entrance of the ejector coming from the condenser unit of a refrigeration system is either a subcooled or a saturated liquid. Inside the motive nozzle, the flow undergoes important pressure variation resulting in a very fast phase change (flashing process) giving turbulent two-phase flow with thermo-dynamical disequilibrium. Even if condensation and evaporation have been studied for several years, many uncertainties about low void fraction two-phase flow and critical conditions remain.

In this paper, a one-dimensional compressible steady state two-phase flow model is presented with new choking criterions that are directly related to optimal flux conditions developed by Dostie *et al.* (2009). As a first step, this model is used to study the flow in the motive nozzle of an ejector.

2. MODELING APPROACH

Fig.1 shows a control volume with boundary a_{kf} moving at a speed $\vec{u}_{kf}$. By supposing that this control volume has two phases separated by boundary a_{kj} moving at a speed $\vec{u}_D$, the evolution of a quantity ψ_k associated at the phase *k* is given by the following integral form of the general conservation equation (Delhaye *et al.* 1981):

$$\begin{aligned}\frac{\partial}{\partial t}\int \rho\psi\, dV = &-\int \rho\psi\,(\vec{u}-\vec{u})\cdot\vec{n}\,dA - \\ &\int \rho\psi\,(\vec{u}-\vec{u})\cdot\vec{n}\,dA - \int \vec{J}\cdot\vec{n}\,dA - \\ &\int \vec{J}\cdot\vec{n}\,dA + \int \rho\varphi\, dV + \int \varphi\, dA\end{aligned} \quad (1)$$

where ρ_k is the density of phase *k*, V_k his volume, $\vec{u}_k$ et $\vec{u}_{kf}$ are velocity of phase *k* and the boundary respectively, $\vec{n}_{kf}$ is the normal vector on the control volume boundary, $\vec{J}_k$ is a tensor, and φ_k is a source term by unit volume of the variable ψ_k.

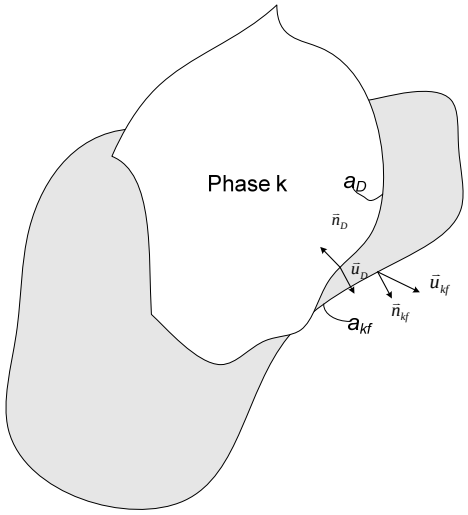

Fig. 1. Diphasic flow illustration.

The one-dimensional conservation equations are obtained using the following substitutions contained in the Table 1.

Table 1 Substitution terms for conservation equations

Equation	ψ_k	$\vec{J}_k$	φ_k	φ_D
Mass	1	0	0	0
Momentum	$\vec{u}_k$	$-\vec{\tau}_k$	$\vec{F}_{ext}$	0
Energy	$e+\frac{\vec{u}\cdot\vec{u}}{2}+\vec{g}\Delta y$	$\vec{q}-\vec{\tau}\cdot\vec{u}$	$\vec{F}\cdot\vec{u}$	0
Entropy	s	$\frac{\vec{q}_k}{T_k}$	$\frac{\Delta_k}{\rho_k}$	Δ_D

where $e+\frac{\vec{u}}{2}+\vec{g}\Delta y$ is the sum of the internal, kinetic and potential energies, $\vec{\tau}_k$ is the strain tensor, $\vec{F}_{ext}$ is the external forces vector by mass unit, $\vec{q}_k$ is the heat exchange vector, and T_k is the temperature of phase *k*. The term $\vec{\tau}_k\cdot\vec{u}_k$ represents viscous dissipation of the kinetic and heat energies, Δ_k is the entropy source by mass unit, and Δ_D is the interfacial entropy source between phases.

2.1. Diphasic Flow Models

While two pressure models shown interesting aspect about two phase flow, none of them have reached a sufficient level of maturity to solve technical and scientific problems. In this model, each phase can have a distinct pressure since the pressure ratio is introduce as a closure law.

Neglecting the influence of heat conduction and viscous dissipation in comparison with mass and energy transfer at the interface between phases, the assumptions for the following air-water model are:

- no viscosity
- adiabatic
- one pressure
- one temperature
- no phase change
- permeable boundaries

For this diphasic flow model, the following conservation equations are used:

$$\begin{aligned}
&\frac{d}{dx} A_k \rho_k u_k = \Gamma_{k,M} + \Gamma^c_{k,M} \\
&\frac{d}{dx}\left(A_k \rho_k u_k^2 + A_k p_k \right) = \Gamma_{k,J} + \Gamma^c_{k,J} \\
&\frac{d}{dx}\left(A_k \rho_k u_k \right)\left(\left(h_k + \frac{u_k^2}{2} \right) A_k \rho_k u_k \right) = \Gamma_{k,E} + \Gamma^c_{k,E}
\end{aligned} \tag{2}$$

where the k indices identify the phase, A_k is the flow area occupied by phase k, ρ_k is the density of phase k, u_k her velocity, p_k her pressure and h_k her enthalpy. The Γ terms are source terms. Subscript c is for boundary terms and M, J and E are linked to mass, momentum and energy source terms, respectively. $\Gamma_{k,M}$, $\Gamma_{k,J}$ et $\Gamma_{k,E}$ represent respectively the transfer term for mass, momentum and energy. At the flow boundary, $\Gamma^c_{k,M}$, $\Gamma^c_{k,J}$ and $\Gamma^c_{k,E}$ are linked to the transfer of mass, momentum and energy. Their formulations are presented in Martel (2012). These equations are equivalent to those habitually found in literature.

Globally, since we face off conservative system, the source terms summation must be null:

$$\sum \Gamma_{k,M} = 0 \,,\ \sum \Gamma_{k,J} = 0 \,,\ \sum \Gamma_{k,E} = 0$$

Since this two-fluid models of two-phase flow are formulated around the macroscopic separate balance equations for each of the two phases, based on space and time averaging of the local instantaneous phasic flow equations, this model can provide information only on the average flow behavior, which assumes that sufficiently accurate empirical correlations can be used to describe heat, mass and momentum transfer processes at the phasic interface and at the boundary walls.

2.2 Closure laws

In this system, we encounter ten unknown, five for each phase: T_k, p_k, u_k, α_k and ρ_k. To close this system, we need two more equation for each phase. First of all, a constant density for incompressible phase and a state equation for compressible phase is introduced:

$$p_k = z_{ck} \rho_k R_k T_k \tag{3}$$

Where z_{ck} is the compressibility factor, R_k perfect gas constant and T_k the temperature of the phase k defined as a function of his enthalpy by assuming that the specific heat is C_{pk} is constant:

$$h_k = h_k^0 + C_{pk}\left(T_k - T_k^0 \right) \tag{4}$$

where h_k^0 et T_k^0 are constant values.

In addition, the following constraints are used:

$$\begin{aligned}
&\sum A_k = A \\
&\sum \alpha_k = 1
\end{aligned} \tag{5}$$

Where α_k is the void fraction defined as a function of total cross sectional area A:

$$\alpha_k = \frac{A_k}{A} \tag{6}$$

These constraints are not linked to a particular phase but to the global mixture. These are global flow conditions.

One more relation is needed to define the flow topology. This equation is often replaced by a correlation linking pressure between phases:

$$p_2 = f(p_1) \tag{7}$$

This correlation can take several forms and the simplest is identical local pressure for each phase. This is the case in this model so we obtain a one pressure model.

2.3 Critical conditions

The critical conditions for this system have been developed by Dostie *et al.* (2009) and presented by Martel (2012). Considering a system with n phases, the criterion is based on global flux terms for mass, momentum and energy:

$$\begin{aligned}
&M = \sum_k A \alpha_k \rho_k u_k \\
&J = \sum_k A \alpha_k \rho_k u_k^2 + \sum_k A \alpha_k p_k \\
&E = \sum_k \left(h_k + \frac{u_k^2}{2} \right) A \alpha_k \rho_k u_k
\end{aligned} \tag{8}$$

By using Eq. (5), the energy flux becomes:

$$E = \sum_k \left(h_k^0 + \frac{C_{pk}}{z_{ck} R_k} \frac{p_k}{\rho_k} + \frac{u_k^2}{2} \right) A \alpha_k \rho_k u_k \tag{9}$$

By scaling each phasic flux by respect to the flux of compressible phase (phase 1), the following scaling factor are obtained:

$$f_{Mk} = \frac{\alpha_k \rho_k u_k}{\alpha_1 \rho_1 u_1}$$

$$f_{J_u k} = \frac{\alpha_k \rho_k u_k^2}{\alpha_1 \rho_1 u_1^2}$$

$$f_{J_p k} = \frac{\alpha_k p_k}{p_1}$$

$$f_{E_h k} = \frac{\alpha_k \rho_k u_k h_k^0}{\alpha_1 \rho_1 u_1 h_1^0} \tag{10}$$

$$f_{E_p k} = \frac{\alpha_k \rho_k u_k \dfrac{p_k}{\rho_k} \dfrac{C_{pk}}{z_{ck} R_k}}{\alpha_1 \rho_1 u_1 \dfrac{p_1}{\rho_1} \dfrac{C_{p1}}{z_{c1} R_1}}$$

$$f_{E_u k} = \frac{\alpha_k \rho_k u_k u_k^2}{\alpha_1 \rho_1 u_1 u_1^2}$$

The mixture flux can now be express as:

$$\begin{aligned} \mathrm{M} &= \mathrm{A}\alpha_1 \rho_1 \mathrm{u}_1 \sum_{\mathrm{k}} \mathrm{f}_{\mathrm{Mk}} \\ \mathrm{J} &= \mathrm{A}\alpha_1 \rho_1 \mathrm{u}_1^2 \sum_{\mathrm{k}} \mathrm{f}_{\mathrm{J_u k}} + \mathrm{A p_1} \sum_{\mathrm{k}} \mathrm{f}_{\mathrm{J_p k}} \end{aligned} \tag{11}$$

$$E = \left(h_1^0 \sum_k f_{E_h k} + \frac{p_1}{\rho_1} \frac{C_{p1}}{z_{c1} R_1} \sum_k f_{E_p k} + \frac{u_1^2}{2} \sum_k f_{E_u k} \right) \frac{M}{\sum_k f_{Mk}}$$

By using the following relation

$$\alpha_1 = 1 - \sum_2^n \alpha_k \tag{12}$$

and the slip ratio

$$s_k = \frac{u_k}{u_1}$$

the phase 1 density can be express by:

$$\rho_1 = \frac{M}{A u_1 \sum_k f_{Mk} - M \sum_2^n \dfrac{f_{Mk}}{\rho_k s_k}} \tag{13}$$

and the pressure by:

$$\mathrm{p_1} = \left(\mathrm{J} - \frac{\sum_{\mathrm{k}} \left(\mathrm{f}_{\mathrm{J_u k}} \right)}{\sum_{\mathrm{k}} \left(\mathrm{f}_{\mathrm{Mk}} \right)} \mathrm{M} \left(\mathbf{1} - \sum_{\mathrm{k=2}}^{\mathrm{n}} \left(\frac{\mathrm{f}_{\mathrm{Mk}}}{\rho_{\mathrm{k}} s_{\mathrm{k}}} \right) \right) \mathrm{Gu_1} \right) \frac{\mathbf{1}}{\mathrm{A} \sum_{\mathrm{k}} \left(\mathrm{f}_{\mathrm{J_p k}} \right)} \tag{14}$$

where

$$G = \left(\frac{M}{\sum_k \left(f_{Mk} \right) A w_1 - M \sum_{k=2}^n \left(\dfrac{f_{Mk}}{\rho_k s_k} \right)} \right) \tag{15}$$

At a singular point, a mixture flux should be an optimum in respect to the primitive variable variations:

$$\frac{dF^{\{Y\}}}{dY} = 0 \tag{16}$$

Where F is a given mixture flux and Y is a primitive variable expressed as a function of mixture flux. For example, Dostie *et al.* (2009) have shown that a local optimum of the momentum flux express as a function of the velocity of the compressible phase 1 and others global flux is given by:

$$\frac{dJ^{\{u_1\}}}{du_1} = \frac{dJ(u_1, M, E)}{du_1} = 0 \tag{17}$$

This equation shows a critical criterion and gives a simple way to know if the flow is critical or not. These critical points correspond to singular points in the differential dynamical system trajectory associated to conservation equations.

The explicit relation for the momentum flux as a function of u_1, M and E is obtained:

$$J^{\{u_1\}} = J(u_1, M, E) = \frac{W}{\left(\dfrac{\sum_2^n \dfrac{f_{Mk}}{\rho_k s_k}}{\sum_k f_{J_p k}} - \dfrac{\sum_k f_{Mk}}{\sum_k f_{J_p k}} \dfrac{A}{M} u_1 \right)} \tag{18}$$

where

$$\begin{aligned} W = &\left(\left(\frac{\sum_k f_{J_u k}}{\sum_k f_{J_p k}} - \frac{\sum_k f_{E_u k}}{\sum_k f_{E_p k}} \frac{C_{p1}}{2 z_{c1} R_1} \right) A u_1^2 - \right. \\ &\frac{\sum_k f_{J_u k}}{\sum_k f_{J_p k}} \frac{M}{\sum_k f_{Mk}} \sum_2^n \frac{f_{Mk}}{\rho_k s_k} u_1 - \\ &\left. \left(A h_1^0 \frac{C_{p1}}{z_{c1} R_1} \frac{\sum_k f_{E_h k}}{\sum_k f_{E_p k}} - A \frac{C_{p1}}{z_{c1} R_1} \frac{E}{M} \frac{\sum_k f_{Mk}}{\sum_k f_{E_p k}} \right) \right) \end{aligned} \tag{19}$$

The following critical condition is then obtained:

$$\frac{\rho_1 u_c^2}{p_1} = \frac{1}{\alpha_1 \left(\alpha_1 \dfrac{\sum_k f_{J_u k}}{\sum_k f_{J_p k}} - \dfrac{\sum_k f_{E_u k}}{\sum_k f_{E_p k}} \dfrac{z_{c1} R_1}{C_{p1}} \right)} \tag{20}$$

where u_c is the critical compressible phase velocity. For a perfect gas, this critical condition is reduced to the sound speed. Otherwise, for a liquid, in which R_k is in the order of 0, the right is equal to 1:

$$\frac{\rho_1 u_c^2}{p_1} = \frac{1}{1 - \dfrac{z_{c1} R_1}{C_{p1}}} \tag{21}$$

This criterion is then valid for compressible as well as incompressible flows. In addition, this local criterion is also valid to the entire flow. The critical

position is obtained when the compressible velocity is equal to the velocity in the critical condition as in single phase compressible flow. The critical condition is defined:

$$DIS = \frac{u_1}{u_c} \geq 1 \tag{22}$$

3. NUMERICAL APPROACH

In this case, a two-fluid one pressure one-dimensional two-phase flow model is obtained. This model takes into account mechanical and thermal disequilibrium between phases as well as phase change. Compressible SIMPLE algorithm from Patankar (1980) is used to solve this system. A constant liquid density and perfect gas law are assumed for incompressible and compressible phases, respectively. In addition, uniform droplets repartition in gas flow for momentum exchange between phases is assumed. With these assumptions, the following six equations model is obtained:

$$\begin{aligned}
&\frac{d}{dx}\sum_k \left(f_{Mk}\right) A\alpha_1\rho_1 u_1 = 0 \\
&\frac{d}{dx} A\alpha_1\rho_1 u_1^2 \sum_k f_{J_u k} + \frac{d}{dx}\left(Ap\right) = p\frac{dA}{dx}
\end{aligned} \tag{23}$$

$$\begin{aligned}
&\frac{d}{dx}\left(\frac{\left(h_1^0 \sum_k f_{E_h k} + C_{p1}T_1 \sum_k f_{E_p k} + \frac{u_1^2}{2}\sum_k f_{E_u k}\right)}{A\alpha_1\rho_1 u_1}\right) = 0 \\
&\frac{d}{dx}\left(A\alpha_2\rho_2 u_2\right) = \Gamma_{2,M} \\
&\frac{d}{dx}\left(A\alpha_2\rho_2 u_2^2\right) + \frac{d}{dx}\left(A\alpha_2 p\right) = \Gamma_{2,J} + \Gamma_{2,J}^c \\
&\frac{d}{dx}\left(A\alpha_2\rho_2 u_2\left(C_{p2}T_2 + h_2^0 + \frac{u_2^2}{2}\right)\right) = \Gamma_{2,E}
\end{aligned} \tag{24}$$

where source terms are:

$$\begin{aligned}
&\Gamma_{2,M} = \frac{N_2 A_{p2} h_M \left(\rho_{y2} - \rho_{s2}\right)}{u_2} \\
&\Gamma_{2,J} = -\frac{A_2}{V_p}\frac{A_{c2}C_D}{2}\rho_1\left(u_2 - u_1\right)\left|u_2 - u_1\right| \\
&\Gamma_{2,J}^c = p\frac{d}{dx}\left(A\alpha_2\right) \\
&\Gamma_{2,E} = \Gamma_2^{Eq} + \Gamma_2^{Eh} + \Gamma_2^{Eu}
\end{aligned} \tag{25}$$

In these equations, $\Gamma_{2,J}$ is the drag term between phases, $\Gamma_{2,J}^c$ is linked to the variable area in a nozzle, $\Gamma_{2,M}$ is the phase change source term, and $\Gamma_{2,E}$ is the energy transfer source term between phases.

This source term can be defined with respect to convective transfer:

$$\Gamma_2^{Eq} = \frac{N_2 A_{p2} h_c \left(T_1 - T_2\right)}{u_2} \tag{26}$$

Where N_2 is the droplet flow rate, $A_{p2}$the droplet cross sectional area, and h_c the convective coefficient. Phase change produce energy and momentum transfer between phases:

$$\begin{aligned}
&\Gamma_2^{Eh} = \Gamma_2^M h_y \\
&\Gamma_2^{Eu} = \frac{u_2^2}{2}
\end{aligned} \tag{27}$$

where h_y is phase change enthalpy.

In this model, only one variable remains for the liquid phase since all other are defined in function of the compressible phase using the scaling factors. In order to take account of the mechanical disequilibrium, the slip ratio between phases must be obtained.

3.1 Slip ratio

To obtain the ratio of the velocity of each phase, phasic momentum conservation equation is used:

$$\frac{d}{dx}\left(M_k u_k\right) + \frac{d}{dx}\left(A\alpha_k p\right) = \Gamma_{k,J} + \Gamma_{k,J}^c \tag{28}$$

where M_k is the mass flow rate of phase k. This mass flow rate is obtained from the mass conservation equation:

$$\frac{d}{dx}\left(M_k\right) = 0 \tag{29}$$

The discretized momentum equation for the phase k is:

$$\begin{aligned}
u_{ki} - u_{ki-1} = &-\frac{\left(A\alpha_k p_k\right)_i - \left(A\alpha_k p_k\right)_{i-1}}{M_k} \\
&+\frac{1}{M_k}\Delta x_i\left(\Gamma_{k,J} + \Gamma_{k,J}^c\right)_{mi}
\end{aligned} \tag{30}$$

with

$$\begin{aligned}
&\Gamma_{k,J} = -\frac{V_k}{V_p}\frac{A_k^D}{\Delta x}\frac{C_D}{2}\rho_k\left(u_k - u_1\right)\left|u_k - u_1\right| \\
&\Gamma_{k,J}^c = p\frac{d\left(A_s\alpha_k\right)}{dx}
\end{aligned} \tag{31}$$

where V_k is the volume of phase k, V_p is the volume of a particle, A_k^D is the cross section area of a particle, and CD the drag coefficient. In this case, virtual mass is neglected.

The pressure terms can be simplified together and the following phase velocity equation is obtained:

$$\begin{aligned}
u_{ki} - u_{ki-1} = &-\frac{1}{M_k}\left(\frac{a_{si}\alpha_{ki} + a_{si-1}\alpha_{ki-1}}{2}\right)\left(p_i - p_{i-1}\right) \\
&+\frac{1}{M_k}\Delta x_i\left(\frac{\Gamma_{k,Ji} + \Gamma_{k,Ji-1}}{2}\right)
\end{aligned} \tag{32}$$

While the phase velocity is obtained, the slip ratio is calculated as follows:

$$s_{ki} = \frac{u_{ki}}{u_{1i}} \tag{33}$$

4. VALIDATION

At the nozzle inlet, a steady state homogeneous flow from a reservoir is supposed. For this reason, each phase has the same temperature and same pressure. The void fraction is imposed at the inlet. At the outlet, the pressure is fixed. Initial conditions in the nozzle are those of the inlet reservoir. This assumption implies a big discontinuity at the outlet for the first step of the numerical solution. To obtain a converged solution, the relative variation of each primitive variable between two iterations must be less than 1x10-6.

The numerical scheme and the model have been validated by comparing some experimental results from Elliot and Weinberg (1968), Lemonnier and Selmer-Olsen (1992) and with numerical results from Städtke (2006). The phase change part of the model has been validated and presented by Martel (2012).

4.1 Elliot and Weinberg

Experimental results were obtained using a 1.27 m experimental nozzle. They presented a pressure profile and mass flow rate in addition of thrust measurement. Inlet conditions are p_0= 10.3421 MPa, T_0=293K and an exit pressure of 0.1013MPa. Fig. 2 shows a good agreement between pressure profiles. For this test, the mass flow rate ratiof_{m2} is 29.1. The experimental mass flow rate is 67.33 kg/s and the numerical mass flow rate is 67.64kg/s for an error of 0.45%.

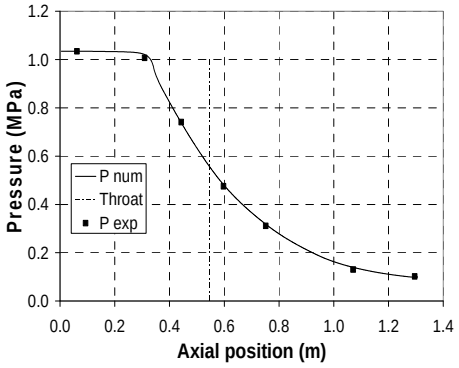

Fig. 2.Pressure profiles in the nozzle.

Table 2 shows experimental and numerical results for mass flow rate ratio between 15.3 and 64.9. For all tests, the error for the mass flow rate is from 0.11% to 2.77%. However the thrust obtained numerically is overestimated from 4.96% to 8.28%. This overestimation comes from frictionless wall assumption and constant slip ratio is used resulting in a higher mean velocity used in the calculation of the thrust. Some tests have shown that using a variable slip ratio instead of a constant slip ratio reduces mean velocity by about 7%.

Table2Comparison between numerical results and experimental measurements

Experimental measurements			Numerical results			
f_{M2}	M (kg/s)	Thrust (N)	M (kg/s)	Error (%)	Thrust (N)	Error (%)
15.3	44.5	6334	45.8	2.77	6748	6.54
17.2	47.7	6236	48.1	0.83	6753	8.28
21.1	51.8	6441	52.5	1.27	6760	4.96
22.3	53.6	6308	53.7	0.14	6762	7.21
28.3	57.7	6308	59.3	2.76	6773	7.38
30.1	60.9	6334	60.8	0.11	6776	6.97
39.1	67.7	6334	67.3	0.59	6760	6.72
51.6	74.5	6334	75.4	1.13	6813	7.55
64.9	81.4	6334	82.2	1.00	6844	8.04

4.2 Lemonnier and Selmer-Olsen (1992)

The nozzle geometry used by Lemonnier and Selmer-Olsen (1992) has a throat with a constant cross-section area. Flow inlet conditions are 0.6 MPa and 292 K with a mass flow rate ratio varying from 27 to 50. Comparison between numerical results and experimental measurements gives an error less than 2% for the mass flow rate.

Fig. 3 shows the pressure profiles comparison. A good agreement is obtained throughout the entire nozzle.

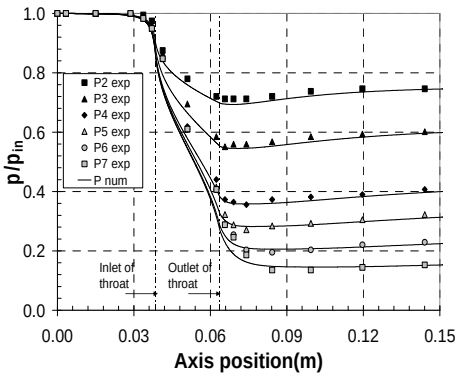

Fig. 3. Pressure profiles in the nozzle.

4.3 Städtke (2006)

The ASTAR nozzle geometry presented by Städtke (2006) is used to compare numerical results. Städtke (2006) used a six equations hyperbolic model with two fluids. For this case, fixed upstream reservoir pressure and temperature of p_0 = 1 MPa, T_0 = 400 K, $u_1 = u_2$ is used with a mass flow rate ratio (f_{m2}) of unity and an exit pressure of 0.6 MPa. Numerical results obtained with this scheme are in good agreement with those of authors as shown on Fig. 4. Total mass flow rate obtained by authors is 5.68 kg/s compared to 5.70 kg/s obtained with this numerical model which implied a difference of 0.35%.

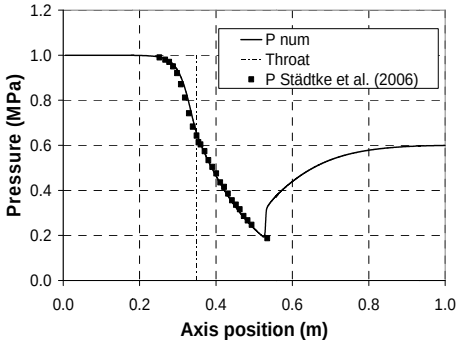

Fig. 4. Pressure profiles in the ASTAR nozzle.

5. NUMERICAL STUDY

Numerical results study is made with ASTAR nozzle and different mass flow rate ratio and exit pressure. Fig. 5 shows the ASTAR nozzle geometry.

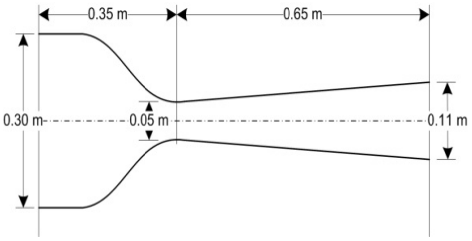

Fig. 5. ASTAR nozzle geometry.

The numerical model is completely independent of the theoretical development and this section will validate this development. For all tests, inlet conditions are: T_0 = 400K, P_0 = 1 MPa, and $u_1 = u_2$. In addition, thermal equilibrium is assumed in the entire nozzle with no wall friction and no exchange (heat and mass) with nozzle walls.

5.1 Validation of the choking criterion

The SIMPLE compressible scheme has been validated with experimental data and previous numerical data from literature. Critical conditions can now be explored using numerical results to calculate choking criterion. These numerical results obtained with the compressible SIMPLE scheme have no explicit link with this criterion. As mentioned before, at a singular point, mixture flux variation express as a function of one dependent variable is 0:

$$\frac{dF^{\{Y\}}}{dY} = 0 \tag{34}$$

Fig. 6 shows numerical mixture variation flux profiles for an air-water flow in the ASTAR nozzle mechanical disequilibrium (f_{M2} = 5, p_{in} = 1 MPa, p_{out} = 0.68MPa, T_{in} = 400 K). It corresponds to a critical flow condition like sonic flow conditions in compressible single-phase flow. These five profiles, calculated using numerical results, are effectively 0 at the critical location. Other four profiles are not shown on this graph for visualization purpose, but they are also zero at the critical point.

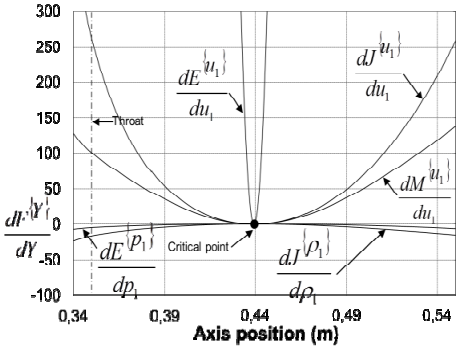

Fig. 6. Mixture mass flow rate through ASTAR nozzle as a function of outlet pressure.

Fig. 7 shows the relative variations of the primitive variables for the previous numerical air-water flow in the ASTAR nozzle. At the critical point, no particular change is observed. The critical point seems to be an anonymous point in regard to the compressible phase evolution. However, this point corresponds to a mixture evolution change from subcritical to supercritical state. In reference to Fig. 6, at this point, the compressible phase cannot modify is state to allow a bigger mass flow rate since:

$$\frac{dM^{\{u_1\}}}{du_1} = \frac{dM^{\{\rho_1\}}}{d\rho_1} = 0 \tag{35}$$

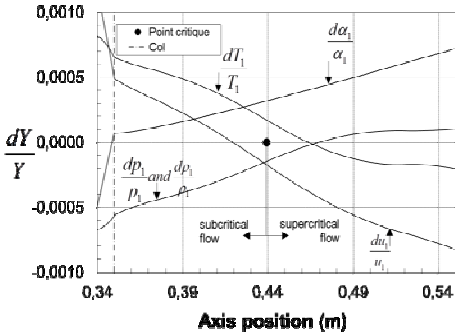

Fig.7. Relative variations of primitive variables.

5.1 Critical location

In single phase flow, critical location is at the throat. However, this is not necessary the case in multiphase flow since mass, momentum and energy exchanges between phases give a different behavior. The critical point may occur in the divergent. Fig. 8 shows critical location as a function of outlet pressure for mass flow rate ratio of 1, 2, 5 and 10. When mass flow rate ratio increases, the position of the critical point get farther of the throat location (0.35 m). Critical location moves upward to the throat position when pressure decreases until an asymptotical value where outlet pressure has no influence on it. In addition, when mass flow rate ratio increases, the minimum critical location seems to reach an asymptotical value.

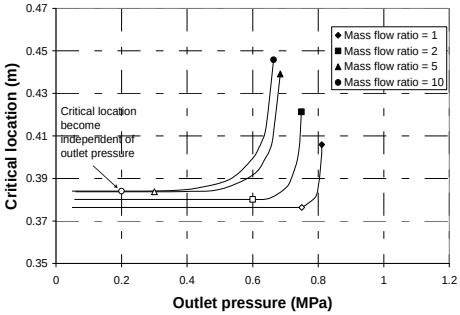

Fig. 8. Critical location in ASTAR nozzle as a function of outlet pressure.

5.2 Critical flow rate with pressure

In single phase compressible flow, when the exit pressure is reduced below a critical pressure, the flow becomes choked and the mass flow rate is maximal. However, in two phase compressible flow, the flow can be critical, but the pressure reduction still has influence on the flow properties until a certain value of outlet pressure – the limit pressure. Fig. 9 shows a complex behavior where the flow can be critical but not necessary choke. This pressure range increases with the mass flow rate ratio as shown in Table 3.

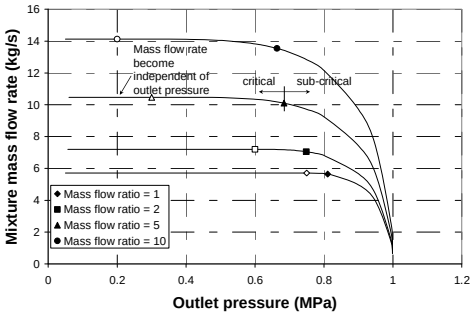

Fig. 9. Mixture mass flow rate through ASTAR nozzle as a function of outlet pressure.

Table3 Difference between first critical mass flow rate and maximum mixture mass flow rate as a function of f_{M2}

f_{M2}	M critical (kg/s)	M max (kg/s)	% diff
1	5.64	5.71	1.24
2	7.05	7.20	2.13
5	10.10	10.46	3.56
10	13.54	14.13	4.36

5.3 Slip ratio influence

The slip ratio has an effect on flow behavior. The use of constant slip ratio results in a sharp discontinuity similar to single phase flow in the divergent section as shown on Fig. 10. In addition, the critical point is at the throat and the critical mass flow rate is defined at this singular point. For a variable slip ratio, behavior is more complex since critical location is downstream the throat and sharp discontinuities are blurred as mass flow rate ratio increases. Transitions between flow regimes are smoother and variable slip ratio allows pressure to decrease as section increases between throat and critical location as shown on Fig. 11. These effects are more marked as the mass flow rate ratio increases. Variable slip ratio allows an increasing of critical mass flow rate when exit pressure decreases up to a limit mass flow rate where properties become independent of exit pressure. Fig. 12 shows the variable slip ratio profiles for different tests conditions.

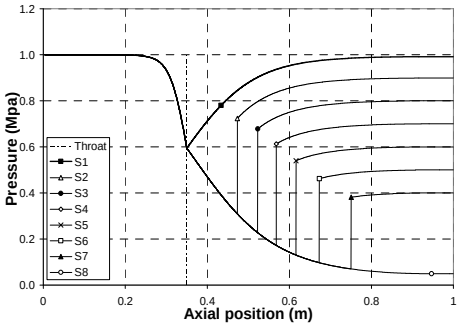

Fig. 10. Pressure profiles in the nozzle with f_{M2} = 10 and constant slip ratio of unity.

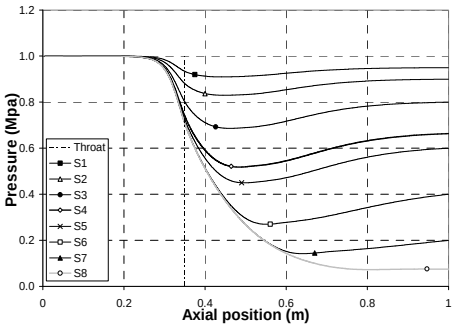

Fig. 11. Pressure profiles in the nozzle with f_{M2} = 10 and variable slip ratio.

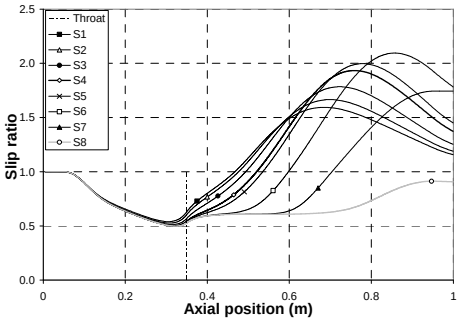

Fig. 12. Slip ratio profiles in the nozzle with f_{M2} = 10 and variable slip ratio.

6. CONCLUSION

Multiphase systems present significant scientific challenges and the choking phenomenon has to be taken into account properly to achieve an accurate

model of two phase ejectors. This paper presents a steady one-dimensional model including new choking criterion based on a new critical fluxes analysis in conservative systems. They provide the information needed to anticipate choking location and critical conditions. It also shows that steady state models are achievable for critical multiphase flows. Such an approach is in some cases simpler than using transient models which involve much more complex propagation phenomenon.

ACKNOWLEDGEMENTS

The work described here was supported by NSERC, FQRNT and NSERC Chair in Industrial Energy Efficiency (chairholder: N. Galanis) at University of Sherbrooke with the support of Hydro-Quebec (Energy Technology Laboratory, LTE), Rio Tinto Alcan and the CANMET Energy Technology Center (CETC-Varennes, Natural Resources Canada).

REFERENCES

Delhaye, J. M., M Giot, and M. L. Riethmullet, (1981).*Thermohydraulics of two-phase systems for industrial design and nuclear engineering*. McGraw Hill, New York, 525 p.

Dostie, M., S. Martel and Y. Mercadier (2009), Critical fluxes in conservative systems: application to multiphase flow. *Personal report*.

Elliot, D. G. and E. Weinberg (1968), Acceleration of Liquids in Two-Phase Nozzles, *JPL Tech. Rep. 32-987*.

Lemonnier, H. and S. Selmer-Olsen (1992), Experimental investigation and physical modeling of two-phase two-component flow in a converging-diverging nozzle. *International Journal of Multiphase Flow 18(1)*, 1-20.

Martel, S. (2012), *Étude numérique d'un écoulement diphasique critique dans un convergent-divergent.*PhD. Thesis, University of Sherbrooke.

Patankar, S. V. (1980). *Numerical heat transfer and fluid flow*, Hemisphere Publishing Corporation, New-York, 197 p.

Städtke, H. (2006), *Gasdynamic aspects of two-phase flow: hyperbolicity, wave propagation phenomena, and related numerical methods*. Wiley-VCH, Weinheim.